ISSN 2303-4521
Periodicals of Engineering and Natural Sciences *Original Research*
Vol. 11, No. 2, April 2023, pp.329-341

The behavior of sandy soils under different types of loading

Reem Siham Tawfeeq[1], Bilal Muiassar M. Salih[1]
[1] Department of Civil Engineering, University of Al-Iraqia, Baghdad, Iraq

ABSTRACT

The method of reinforcement soil layers was acommon technique to improve the ability of the soil to retain load and reduce settlement. Thetechnique has been somewhat dependent, whereas, in the past, there was research on this method of design and analysis. So, soil improvement by reinforcing it must be analyzed correctly. The capacity of assuming the improved bearing capacity underground of reinforced sand was investigated through the user's use of the test executor in diverse test cases. Here in this investigation, four various kinds of reinforcement materials have been used. Four circular models with different interior diameters were used to examine the effect of the circular ratio on the bearing capacity of the soil layer along the various reinforcing state of affairs. A typical plate load test was carried out with the presence of monotonous and periodic loading in three chains mentioned in tests of the monochrome plate loading on ringing base anchoring on layers of sand which are reinforced over Netlon CE121 Geo-grid as a material of reinforcement- 15 numbers, tests of periodic plate-load PLT along Geogrid (Netlon CE121) as materials of reinforcing - 15 number, the Monochromatic tests of plate-load over Geojute as a reinforcing material - 9 number, tests of periodic plate-load PLT over Geojute as a reinforcing material - 9 number.

Keywords: Sandy soil, Reinforcement, Geogrid, Periodic, Monotonous.

Corresponding Author:

Reem Siham Tawfeeq
Department of Civil Engineering
University of Al-Iraqia
Baghdad, Iraq
E-mail: engreemsiham86@gmail.com

1. Introduction

Since civilization's beginning, man has been aiming to use the soil with other materials for future uses. The houses constructed and the way on reinforced soil with fiber and building earthen walls over various kinds of reinforced intrusions is an ancient notion. In the last few years, fibbers and membranes, often called 'Geotextiles and Geomembranes', have been abundant in soil reinforcement to develop their behavior and features [1]. Together with the literature, one finds several techniques to improve the ground based on the soil type and economic viability. The major objective of any method of soil improvement techniques is to reduce the settlement and to develop the bearing capacity. In the current script, soil reinforcing is utilized to make the soil system flexible and plastic. Therefore it can have improved damping properties under the action of the loading periodic or dynamic [2]. The reinforcement soil consists of a mixture of ground and reinforcement components. In-ground, the stress is internally generated by applying frictional forces between the reinforcement material and the dirt, and the anxiety is transferred to reinforcing those materials [3]. Subsequently, the reinforcing material resists parallel error occurrence and adopts the material transmission limit. The main points of geogrids are that a gap between transverse and longitudinal sides is bulky enough to allow the dirt from one hand of the geogrid to the other side [4]. The Reinforced ground is compound improvement material since the building backfill quality is upgraded by an expansion of rigid and non-extensible flexible support [5]. Suppose an overview of the reinforcement in the soil is taken. In that case, one can find that the reinforced soil consists of a group of basic elements, on top of which is the calculated friction force between the dirt and the fortification. These forces exist between the parts of the dirt, which explains the practical balance and the improvement in soil quality. To unify the soil mass in all directions along the places of weakness and potential failure, soil reinforcement adds the characteristic of strength to the soil composition [6]. The reinforced ground is probably

such multi uses. The foundations are distinguished arbitrarily from slabs by the reality they are purposed for loaded supporting areas, which, compared to the reinforced plan areas, is considered small compared to the reinforcement walls. A few research and even lesser structures have been achieved. The reinforced ground has been a method that has attracted many engineering scientists in the region due to its economy of all that is easy to deal with conditions, and the simple lack, over the two past decennium [7]. However, we have yet been able to manage the static loads applied to the soil. The application of these heaps is made gradually, and the increments of their size are through the bit. They don't keep up consistently with the times. Most structures undergo, during their lifetime, many load modifications, even conventional ones [8]. Usually, tall circular structures and ring foundations are provided for it, such as smokestacks, towers of water, silos of cement, etc. The ring foundations are favorite for these structures because of the full employment of the soil capacity and minimal tension under the foundations. In the towers of water, the foundations are under the influence of the periodic load due to the difference in water level [9]. Periodic loading may make a few of them unrecoverable, that is, a plastic strain. Using overburden means we are giving the vital for the soil, which produces strain. In the state that the strain evaporates when the burden is additionally discharged, we have restored vitality. Miss Hapening's plastic enhancement displays that the vitality conferred through loading has been missed or diffused and can be said to have been transformed into plastic deformation [10]. Losing vitality in the soil is named hysteretic or physical damping off. The idea of vitality has been identified by [11], along with deciphering the results of periodic triaxial and total-section tests on oceanic Champlain soils in the Ottawa River Valley region. Numerical connections were established to depict the various parts of dynamic behavior. The study on the mineral by specialists shows that the loading pattern corresponds directly to the cycle vitality level and is independent of where in the chronological history this specified load periodic is applied [12, 13]. In this way, the absolute damage possible under periodic loading is logically determined by the applied length of total vitality. These realizations show that the dirt's possible damage with periodic loading can be depicted by the vitality dispersed in the dirt during loading. The reason for achieving this relationship is due to the method that is being both the scattering vitality and dirt fouling capacity are scalar quantities and can be collected during loading is doing [14]. In addition, the collection of vitality is not affected by the loading-to-frustration method. Its use for imaging dynamic soil behavior may lead to direct, direct correlations [15, 16]. During the past two decades, a few factors have demonstrated the positive effects of using planar supports for sand-bearing boundary construction. Immunization of Geocells is one of the recently established strategies in gabion support [17]. This is a three-measurement, polymerically, as cells of honeycomb construction that are interlinked at joints. The support system is implemented in geocells by the comprehensive dirt containment within their pockets [18]. Unlike fortifications that planar, geocell containment minimizes the spread that parallels internal infill and thus builds on the nature general that is non-convoluted of the reinforced layer. Because of the nature inelastic of the geo-pad, the balancing load distributes along a wider area resulting in a significant improvement in behavior [19]. The geocell bed captures potential explosive planes, and its natural irregular force cuts the planes into the facility's soil, resulting in higher tolerance limits[20]. They led the progress of the model plate load test (PLT) on roundish plinths supported on top of square frame paper full of sand soil to identify different ways for frustration and emerge in cell ideal elements [21]. Strengthening soil strata to improve the mound transport restricted to soil and reduce the settlement [22]. The model is not fully abused since there are no widely accessible tests regarding structure and screening strategies. Along these ranges, there is a requirement to understand soil support connections. The suitability of the "bear limit increase" anticipation strategy in sandy ground reinforced by the constructor is examined using tests conducted under various test cases [23]. In the current study, four different kinds of basic materials were utilized. In circular bases with different inner diameters, 4 models were used to examine the effect of the circular ratio on the sand layer's bearing capacity along various reinforcement conditions [24]. In this article, it has presented in Sec. 2, the work related to methods for predicting the bearing capacity of reinforced sand beds explained, Sec. 3, a discussion of research techniques and methods in Sec. 4, is presented an analysis of results and discussion, Sec. 5, is presented conclusion and work of future.

2. Literature review

This section presents several discussed methods for predicting the bearing capacity of an augmented sand bed with the presence of periodic and monotonous loading of prior studies. Kumar S. S. et al. [1] illustrate predicting a cause of restricted bearing for gradual soils requiring the incremental field test program. The authors suggest authentic relationships to predict reasonable bearing limits and elastic settlement for shallow structures in

granular soils. Existing joints using only standard inlet stroke check number and unit weight of the soil can achieve bearing limit estimation. Mittal R. K et. Al. [4] illustrated that the test results indicate the benefits of geosynthetics completely minimizing the cavitation of the asphalt. Along with two layers of folded geosynthetics, the test segment performs much better than every other segment currently concentrated. The geosynthetics placed at the interface of the underlying subgrade act more as a weak modification of the subgrade than as a reinforcement of the underlying layer for the time being. Test regions are equipped with various sensors to determine the reaction and implementation of the relevant asphalt. Cardile G. et al. [5] presented SRHDPE pipe, which is expressed as another type of road pipe used for waste due to the doubtless dotes of attention, for an instant, great corrosion hindrance and the light weight. In some undertakings, it is covered shallowly. To investigate the effects of a superficially covered funnel on an occurrence of permanent street surface loss under periodic loading of traffic, two tests were directed to the non-paved road research facility across a covering proposed pipe, with the effect of the periodic loading. SRHDPE pipe, 610mm wide, was encased in a compressed sand canal secured by aggregate courses or base of sand in two tests, 1 and 2, each separately. Elleboudy A. M. et al. [8] depicted the achievements of the geographical group for rocky roads subjected to the repeated load(s) discovered while testing the center of research in Shubra and examining the limited components. Twenty-two tests of the research facility model were carried out under periodic loading in street regions consisting of the underlying cycle layer along and without the support of the geo-matrix overlaid on a weak sublevel. The investigated parameters included base bed thickness, grid aperture size, geo-frame stiffness, the layers of several geo-matrix, and geogrid area. Hegde A. et al. [10] illustrate the effects produced beyond the model of the center of research examinations and the guided tests in the square equilibrium placed on clay and sand layers reinforced with geocells. Using suitable scaling reflections, the equilibrium size of the model has appeared from the generation floating model. Industrial access polyethene geocells that have a similar sinusoidal distance of 0.25 m and an angle ratio of 0.6 were used in the experimental screening. To fill the pockets of the geocell, clean sand was used in both the clay and sand tests. Hegde A. et al. [11] presented ordering the results of the research panel's periodic test of the load(s) conducted in the sensitive, reinforced layers. The exhibits of reinforced layers of earth along geocells and geocells contrast along additional geo-basal lattice states and widths of unreinforced dirt layers. From the periodic plate loading test results, the elastic uniform compressive modulus (C_u) was obtained for the different cases. C_u estimation was found to increase, given the geogrid cell reinforcement. Hegda A. et al. [12] depict the following effect(s) of the center of research paradigm investigations and the numerical investigation(s), which leads to the small distance through PVC plastic pipes in touch with the sand layers reinforced with ground cells. The examination aimed to estimate geocell reinforcement's plausibility in saving utilities underground and the covered pipelines. Despite the geocells, additional consideration was given to the feasibility of the geo-cell and geo-lattice only along additional basal genoframe states. Mamatha K. H. et al. [17] show the results of recompiled load tests on unreinforced asphalt regions and ground cells. Typical asphalt areas were worked into a (2 x 2 x 2) m steel tank. The development of the stage has been received during the development of asphalt regions. A Geocell bed was contemplated for the fluctuating angle ratio. The geocell bed was mapped at the sub-bed interface and the granular sub-core course beds in all geocell-reinforced asphalt regions. It is the loading requirement adopted to re-create the loading of vehicles. Pokharel S. K. [18] presented geocells, one type of geosynthetics made into a type of cells that are 3D interconnected, calculated to give a suitable horizontal funnel for filling material to extend the modulus and limit the bearing of the core courses. Most tests have been conducted on the behavior of geocell-reinforced bases under static loading. Geocells used in asphalt usage are subjected to continuous loading. Restricted tests were performed to explore the width of geocell-enhanced bases under continuous loading. Sahu R. [19] depicted free vibration tests performed on a typical reinforced and unreinforced counterbalance. The sand has been reinforced along humane hair fibers and geogrids (PET and HDPE). The merging of fibber had expressed to be $\frac{1}{2}$ % by loading the dry sand. The layer of sand has packed in eight layers, and every layer was consolidated to achieve the ideal relative thickness (80%) using an aligned plate vibrator. Free vibration trials were performed in a typical trial tank by shifting the supported depth (d_r) by keeping the fortification width (w_r) constant. Venkateswarlu H. et al. [23] present the results of massive field experiments and numerical tests conducted on synthetic earth-reinforced soil layers supporting the creation of a prototype machine. A series of vertical position square rebound tests are carried out via an inelastic rigid balance placed on different conditions of the reinforced soil. Tests are carried out in a test pit measuring 2m x 2m x 0.5m using a steel balance measuring 0.6m x 0.6m x 0.5m. Wang J. Q. et al. [24] discussed the properties of dynamic reaction and settlement for the shallow square feet on sand reinforced with a geo-grid under periodic loading.

Seven arrangements of massive scale research center tests were carried out on a 0.5 square meter wide scale on an unreinforced and geo-grid reinforced sand containing steel tank 3m x 1.6m x 2m (L x W x H). Characteristic reinforcement schemes are considered in the tests: one bed of support at a depth of 0.3B, 0.6B, and 0.9B, where B is the width of the scale; two beds and three beds of fortification in-depth and split both at 0.3B.

3. Methods

The utilized soil was defined, and its engineering characteristics were considered in the laboratory by evaluating different tests for periodic and monotonous loading.

3.1. Granular Analysis Phase

The sifting was made by organizing the different sieves, one on top of the other in their working order, opening the largest retained gap screen at the top and a smaller gap screen at the base. The tester has been placed on the upper sieve, and a whole batch has been installed in a sieve vibrating machine. The mentioned vibration has been done for about 10 min. A soil test portion has been performed over every sieve that has been measured. The average soil retained over every sieve has been evaluated depending on the total mass taken hold and the result(s). The average that passes out of the strainer has been computed. In Table 1, perception and appreciation have been shown. Then, the passing rate and grain size graph was plotted. Dim_{10}, Dim_{30}, and Dim_{60} estimates were determined from the flowchart. The coefficient of uniformity (Cu) and coefficient of the shape (Cc) have been evaluated as shown in eq. (1) and (2).

While:

$$Cu = \frac{Dim_{60}}{Dim_{10}} \quad (1)$$

$$Cc = \frac{(Dim_{30})^2}{Dim_{60} . Dim_{10}} \quad (2)$$

Table 1. Sieve granular analysis [3]

Sieve No.	Object(s) Dim	Mass Performed	% Performed	Achieved Accumulative	Aggregative Finer
4.75	4.74	0.00	-	-	100.00
2.36	2.35	1.45	0.14	0.14	99.84
1.18	1.17	333	33.3	33.54	66.44
600.00 µ	0.5	358	35.8	69.44	30.54
300.00 µ	0.28	271	27.1	96.64	3.34
150.00 µ	0.14	27	2.70	99.3	0.59
75.00 µ	0.074	5.9	0.59	100.00	0.00

Note: Dim: (mm), mass: (gm), Accumulative: (%), finer: N

The distribution curve of the particles size

Dim_{10}=0.360

Dim_{30}=0.600

Dim_{60}=1.100

Cu=3.050

Cc=0.910

Soil: SP (Soil Poorly-graded)

3.2. Gs phase

This article's term (Gs) refers to the phase of Specific-Gravity of soil. A pycnometer dry and clean has been taken for testing. The tare pycnometer weighted (W) was completed, and nearly 200-400 gm of kiln-dried sandy soil was transferred for the pycnometer meter. In addition to dry soil, the weight of a meter pycnometer (W_2) has been taken. Then distilled water was added to a pycnometer, measured to half its height and mixed along a glass bar. More water is added up and mixed well. Pycnometer has been filled, To the top of the conical cap along with water. Pycnometer after the drying has externally recorded with the weight (W_3) emptied, cleaned thoroughly, and filled to the top of the conical cover opening with distilled water and the weight recorded as (W_4). Specific gravity Gs determined by utilizing eq. (3) as the following:

$$G_S = W2 - W1/[(W4 - W1) - (W3 - W2)] \quad (3)$$

Table 2. Specific gravity (G_S)

#	Definition	W (gm)
1	weight (the pycnometer) W_1	449
2	weight (the pycnometer + Dry sand) W_2	866
3	weight (the pycnometer + Dry sand) W_3	1679
4	weight (the pycnometer + water)	1423
5	The soil Specific Gravity (G_S) = 2.590	G_S =2.590

3.3. Relative-density (rd) phase

(γd_{min}) = 15.300
(γd_{max}) =18.030
keep field density along the test process: γd = 16.70
while γ is measured in kN/m^3

$$R_d = [(\gamma d - \gamma d_{min})/(\gamma d_{max} - \gamma d_{min})] \times [\gamma d_{max}/\gamma d] \times 100 \quad (4)$$

Then:
R_d = 55.37%
Therefore, the representation samples fall under the medium-density class. The properties of the sand used under the test are shown in Table 3.

3.4. Direct-shear test phase

A shear modulus for a representant soil with a density the same (16.70 kN/m3) utilized in loading tests typically was determined utilizing a square test of the direct shear. The shear components specified after the diagram graphing of normal stress shear stress versus shear stress are as follows:
Cohesion-Coefficient (C) = Zero
Friction-Angle (θ) = 36.
The properties of sand used under investigations are shown in Table 2.

Table 3. Sand Parameters

Gravity	g	2.6
Max. density	γ_{max}	19
Min. density	γ_{min}	16.3
Density	γ	18
Coefficient- Curvature	Cc	0.99
Uniform- Coefficient	Cu	4
Cohesion	C	0
Friction-Angle	θ	42.9

Materials utilized to reinforce the prediction of the bearing capacity of the sand layer in the presence of periodic and monotonous loading, as shown in Table 4.

Table 4. Types of reinforcement materials were used in the investigation

Geo-grids-(Netlon)	CE121	CE131	Measured Unit
Thickness on node(s)	2.750	5.500	mm
Thickness on rib(s)	2.200	2.500	mm
Aperture Dim	7.50 by 7.50	28 by 28	mm
Tensile-stress	7.680	5.800	N/mm
Yield-stress	6.800	5.200	N/mm

3.5. **Analyses of the practical part**

The analysis includes monotonous and periodic sample tests achieved under the ring base setting on the sand over reinforcement layers such as Geogrid CE121 and Geo-jute.

Factors which are following have been studied for each of the materials reinforcing planar:

i. Place the top layer of reinforcement, giving a foot form, u,
ii. Number of reinforcement layers, No., * spacing that Vertical, under the adjacent layers, z,
iii. The reinforcing material(s) size, i.e., (b).

Foot-model utilized in sequence here was circular with an inner Dim (d_{inner}) = 50 mm and an outer diameter (d_{outer}) = 130 mm. As previously defined, the parameters u and z have been kept constant, which equals 0.25 d_{outer}.

3.5.1. PLT along monotonous loading

When the experimental layout is finished, the load has utilized under accumulative equivalent reinforcement until 15 estimations of efficient bearing capacity. The load applied, excluding impact, eccentricity fluctuations, and load on the test loop, was calculated. Settlements were analyzed for each load increment after the settlement rate became minimal. The next load improvement after that was the application and retention of the analysis. A test was performed in which settlement was achieved at 10% of the foot volume or failure of the soil layer under the shear. For all monotonous tests, the settlement versus load curves has been plotted. The effective load bearing stress (q_o) of reinforcement sand was computed along the effective bearing stress of sand, which reinforced q and ($BCR = \frac{q}{q_\circ}$) was calculated. A factor of settlement ratio (SRF) was used to represent the decreased settlement of the reinforced statues. (SRF = S/S_o), thus S = the settlement of the reinforced status on the stress of the bearing identical to the bearing stress, which is effective of unreinforced sand, and the symbol S_o is expressed as the identical settlement to the bearing burden, which is effective of the unreinforced status. The relation between compression and the settlement, which is obtained from tests, was studied by drawing curves for all series of tests performed.

3.5.2. Cyclic PLT

After organizing the arrangement, the readings essential for dial scales have been noted, and the static load's initial addition has been applied to the balance. Heap has been maintained consistently until no further settlement happened or the frequency of the settlement became unimportant. Then the readings, the final of the dial gauge, were recorded. At the point when no additional bounce occurs, or the bounce frequency becomes unimportant, dial gauge readings were noted again. Then step by step, the heap was expanded until its greatness got a value equivalent to the next proposed higher loading stage, which has been kept constant and the last readings of the dial check have been recorded as indicated before. Then the whole load was reduced to zero, and the final dial check readings were recorded when the bounce frequency became irrelevant. The loading, unloading, and reloading patterns continued until they reached the productive load estimated, and each time, the final estimates of dial check readings were noted. The periodic plate loading tests on arranged layers have been directed to test the influence of the above factors on the sand layer's damping limits. The curves of load versus settlement were plotted for each test group. The typical curve of the loading and settlement is shown in Fig. 1. Also, a curve for W* versus S* for every group of loading and unloading has been plotted. After that, the deceleration loops for the test series were obtained. Determining the significance of damping capabilities for the sand reinforced and unreinforced is by calculating the area for the single hysteresis loop and the area beneath W* versus S* along a plot aid scale.

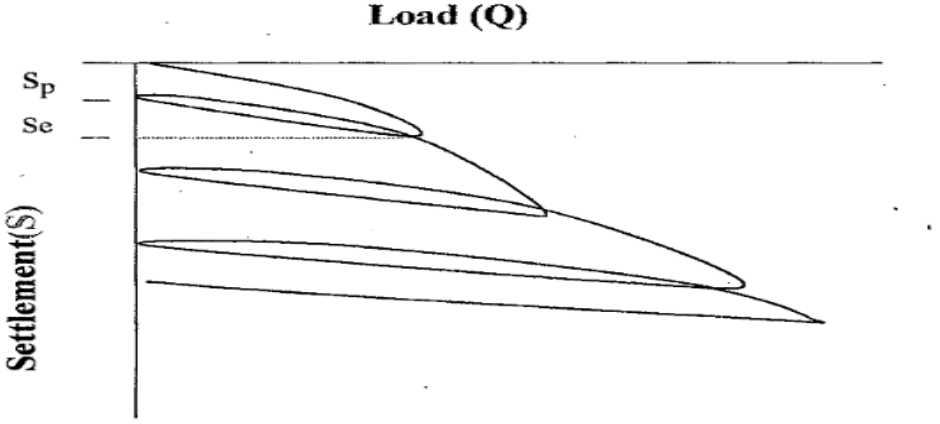

Figure 1. Load and settlement of cyclic PLT

The AU/UO ratio obtained the damping capability index
While

AU = Deceleration loop area,
UO = The area beneath W* versus. S*,
W* = parameter of the Load [p *1 + (γ * dim. $_{outer}$)],
S* = The settlement parameter (S *1 + dim. $_{outer}$),
dim. $_{outer}$ = The out diameter for the circular footing.
p = Intensity of load
γ = Soil density

For each test, loading and the unloading performed made it possible to separate the recoverable S_e component and the component that was not recoverable S_p from the total base settlement of different loading levels. A modulus uniform elastic for C_u in eq. (5), the elastic-shear modulus C_∞, the modulus of uniform elastic shear $C_£$, and the modulus of uniform elastic compression $C_¥$ were described after that by the given communication such as IS – 5249 -1992.

$$C_u = \frac{p}{Se} \quad (5)$$

While

p = corresponding load intensity, by (kN/m^2).
Se = the defection settlement corresponding elastic.
C_u= 1.5-2 $C_¥$,
C_∞ = 3.46 $C_¥$,
$C_£$= 1.5 $C_¥$.

The lab plate loading tests PLT were carried out under monotonous and periodic loading conditions on the sand layer reinforcing along the geocells of various sizes at the 3rd series.

a) The depth of the upper layer of the geocell beneath the base of model, Z
b) Geo-cell diameter of, Dim_g
c) Geo-cell height, mercury, f
d) Geo-cell number No.

Here in this series, it has been used a ring has a diameter that outer (d_{outer} =130.0 millimetres) and an inner diameter (d_{inner} = 50.0 millimetres) as a footing of the model. The tests of plate loading have been performed under the monotonous and periodic loading as depicted in Sec. 3.3.1. Plate-loading tests details performed along the geocell reinforcing are as follows:

a) Tests of monotonous plate loading PLT on the Geocell (of CE121 geogrid) reinforced sand layer with Dim_g = 0.27 d_{outer} (35 millimetres) along No. (l, 2, 3), Hg=0.6 d_{outer} (80 millimetres), the Geo-cells along Z (0.25 d_{outer}, 0.5 d_{outer}, 0.75 d_{outer}), and periodic plate loading tests along the same scales of the geocells and the arrangement group along No. (1 to 4).
b) Tests of monotonous plate loading PLT on the Geocell (of CE121 geogrid) reinforcement sand layer having Dim_g = 0.46 d_{outer} (60 millimetres) along No. (l, 2, 3), Hg=0.6 d_{outer} (80 millimetres), the geo-cells along Z (0.25 d_{outer}, 0.5 d_{outer}, 0.75 d_{outer}), and periodic plate loading tests along the same scales of the geocells and the arrangement group along No. (1 to 4).
c) Tests of monotonous plate loading PLT on the Geocell (of CE121 geogrid) reinforcement sand layer having Dim_g = 0.78 d_{outer} (100 millimetres) along No. (l, 2, 3), Hg=0.6 d_{outer} (80 millimetres), the geo-cells along Z (0.25 d_{outer}, 0.5 d_{outer}, 0.75 d_{outer}), and periodic plate loading tests along the same scales of the geocells and the arrangement group along No. (1 to 4).
d) Tests of monotonous plate loading PLT on the Geocell (of CE121 geogrid) reinforcement sand layer having Dim_g = 0.27 d_{outer} (35 millimetres) along No. (l, 2, 3), Hg= d_{outer} (130 millimetres), the geo-cells along Z (0.25 d_{outer}, 0.5 d_{outer}, 0.75 d_{outer}), and periodic plate loading tests along the same scales of the geocells and the arrangement group along No. (1 to 4).
e) Tests of monotonous plate loading PLT on the Geocell (of CE121 geogrid) reinforcement sand layer having Dim_g = 0.46 d_{outer} (60 millimetres) along No. (l, 2, 3), Hg= d_{outer} (130 millimetres), the geo-cells along Z (0.25 d_{outer}, 0.5 d_{outer}, 0.75 d_{outer}), and periodic plate loading tests along the same scales of the geocells and the arrangement group along N (1 to 4).
f) Tests of monotonous plate loading PLT on the Geocell (of CE121 geogrid) reinforcement sand layer having Dim_g = 0.78 d_{outer} (100 millimetres) along No. (l, 2, 3), Hg= d_{outer} (130 millimetres), the geo-

cells along Z (0.25 d_{outer}, 0.5 d_{outer}, 0.75 d_{outer}), and periodic plate loading tests along the same scales of the geocells and the arrangement group along No. (1 to 4).

g) Tests of monotonous plate loading PLT on the Geocell (of CE121 geogrid) reinforced sand layer with Dim_g =0.27 d_{outer} (35 millimetres) along No. (l, 2, 3), Hg=1.38 d_{outer} (180 millimetres), the geo-cells along Z (0.25 d_{outer}, 0.5 d_{outer}, 0.75 d_{outer}), and periodic plate loading tests along the same scales of the geocells and the arrangement group along No. (1 to 4).

h) Tests of monotonous plate loading PLT on the Geocell (of CE121 geogrid) reinforced sand layer with Dim_g =0.46 d_{outer} (60 millimetres) along No. (l, 2, 3), Hg=1.38 d_{outer} (180 millimetres), the geo-cells along Z (0.25 d_{outer}, 0.5 d_{outer}, 0.75 d_{outer}), and periodic plate loading tests along the same scales of the geocells and the arrangement group along No. (1 to 4).

i) Tests of monotonous plate loading PLT on the Geocell (of CE121 geogrid) reinforcement sand layer having Dim_g =0.78 d_{outer} (100 millimetres) along No. (l, 2, 3), Hg=1.38 d_{outer} (180 millimetres), the geo-cells along Z (0.25 d_{outer}, 0.5 d_{outer}, 0.75 d_{outer}), and periodic plate loading tests along the same scales of the geocells and the arrangement group along No. (1 to 4).

4. Results and discussions

The test results were used to predict the bearing capacity of the reinforced sand layer in the presence of periodic and monotonous loading in the cases of single and periodic loading on the reinforced sand layer along geocells of different sizes in 3rd series. Here, in this series, various parameters are as follows.

a) The geocell top layer depth, below the foot of the model (Z)
b) Geo-cell diameter (Dim_g)
c) Geo-cell height, mercury (Hg)
d) Geo-cell number (No.)

The test results of the monotonous load test of the sand layer reinforced with geocells are presented as follows:

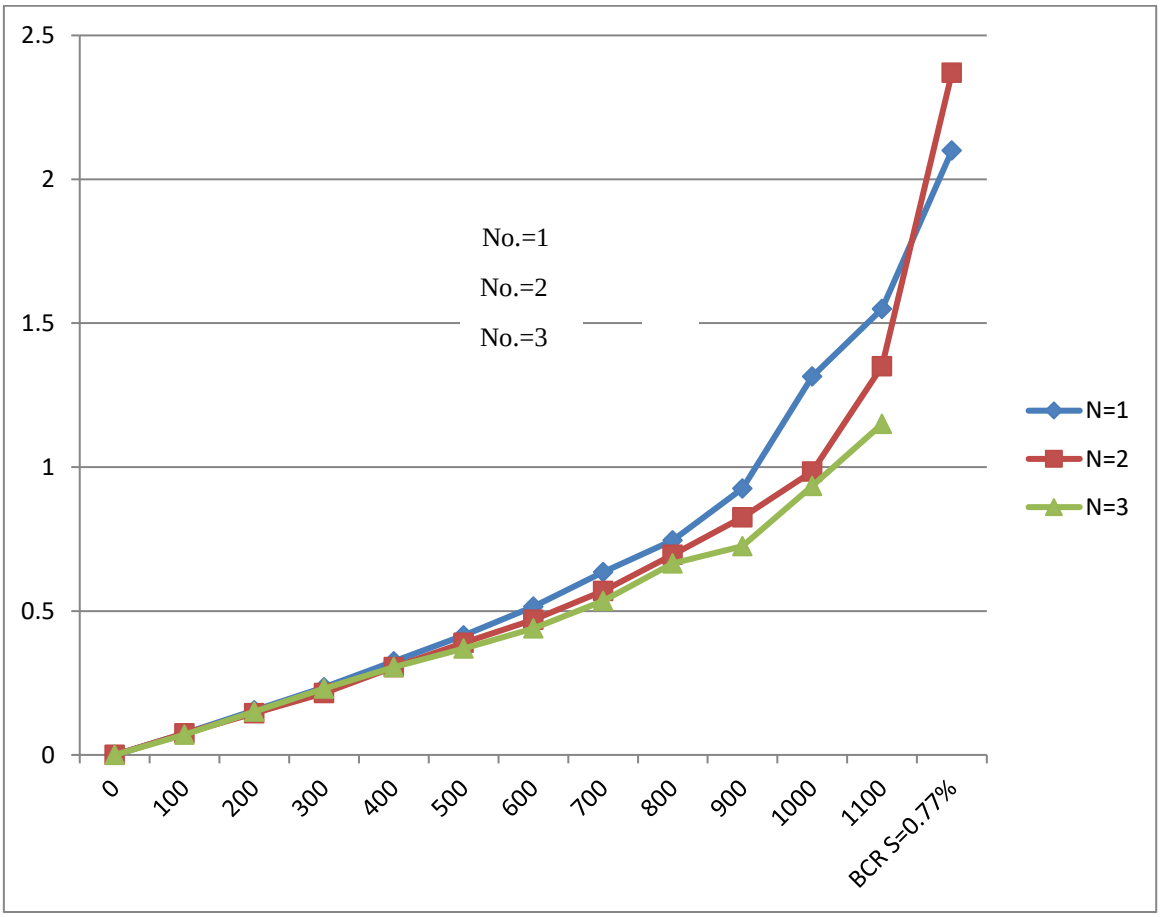

Figure 2. Reinforce layer along geocells ($\frac{z}{d_{outer}} = 0.250$) monotonous load

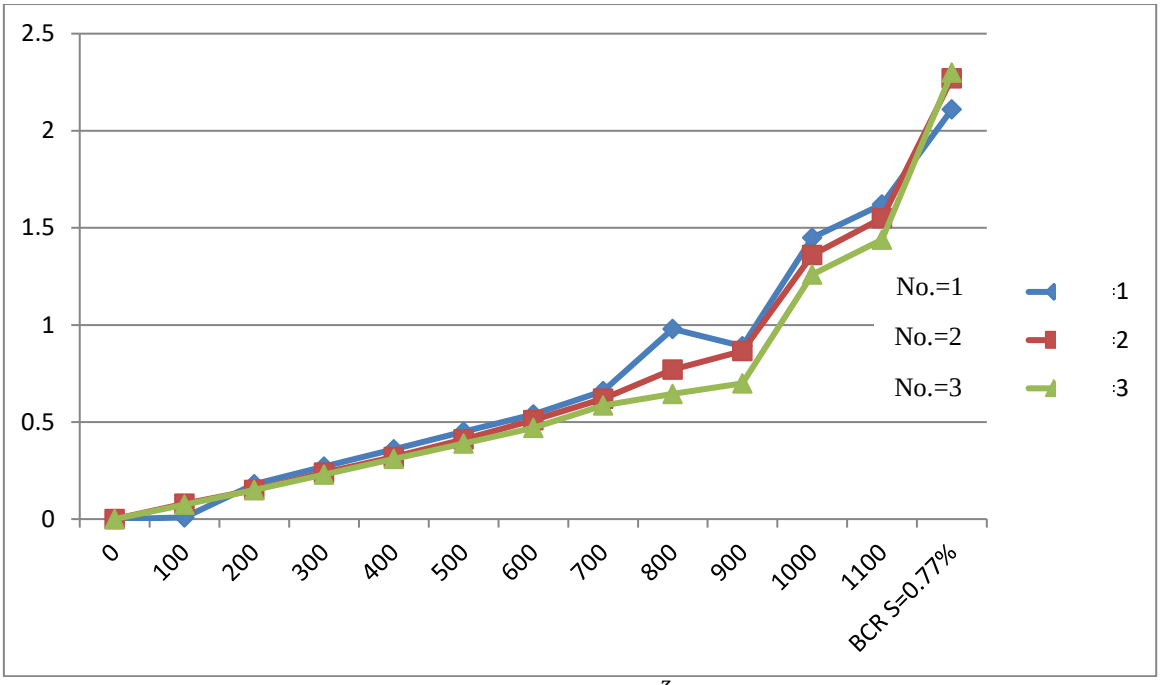

Figure 3. Reinforce layer along geocells ($\frac{z}{d_{outer}} = 0.50$) monotonous load

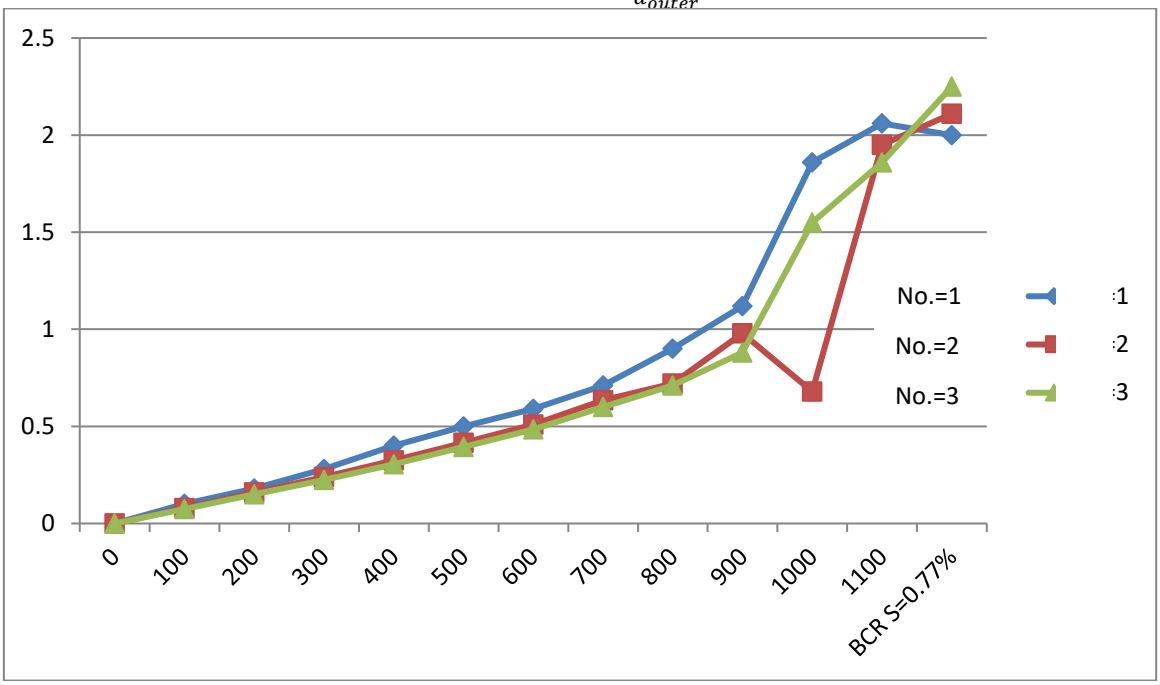

Figure 4. Reinforce layer along geocells ($\frac{z}{d_{outer}} = 0.750$) monotonous load

The figures above were used to experiment with the same sand and density along the reinforcing materiality as geocells. The sand layer has been reinforced along the geocell made of along the Netlon geogrid (CE-121) with diameters for geocell Dim_g (0.27 d_{outer}, 0.46 d_{outer}, 0,78 d_{outer}) which are (35, 60,100 millimetre), with the height of Geo-cell Hg (0,61 d_{outer}, d_{outer}, 1.38 d_{outer}) which are (80, 130, 180 millimetres), with placement depth Z (0.25 d_{outer}, 0.5 d_{outer}, 0.75 d_{outer}) and with a length of geo-cell number No. (1, 2, 3). All results of predicting the bearing capacity of a sand layer in the presence of monotonous loading are shown in Fig. 2, 3 and 4. The results of the test for the periodic PLT on the geocell reinforcement sand bed are as follows:

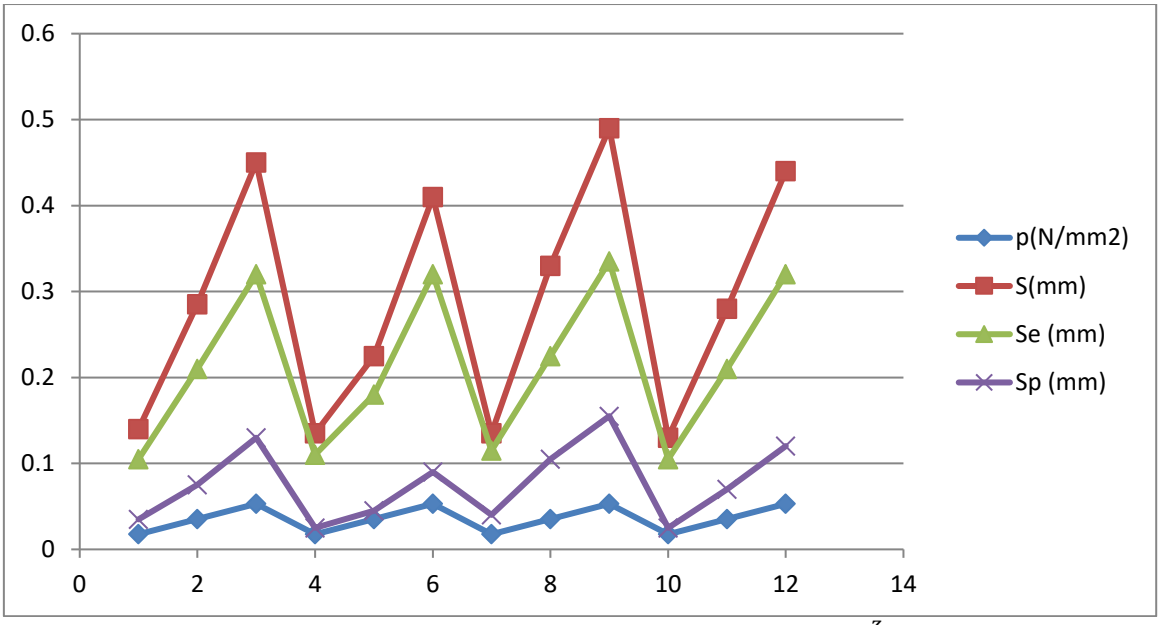

Figure 5. Periodic PLT on geocell reinforcement sand layer ($\frac{z}{d_{outer}} = 0.250$)

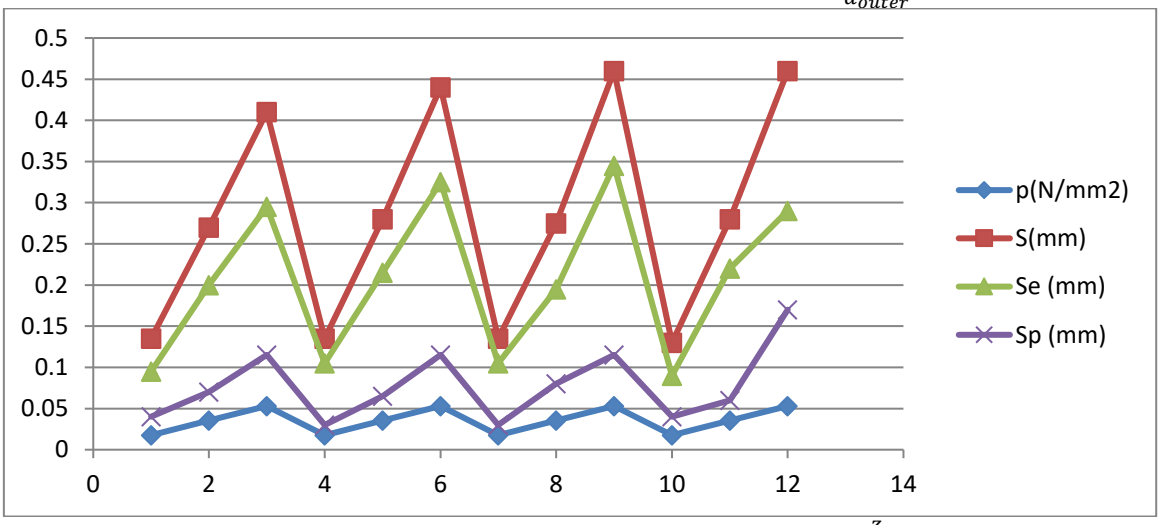

Figure 6. Periodic PLT on geocell reinforcement sand layer ($\frac{z}{d_{outer}} = 0.050$)

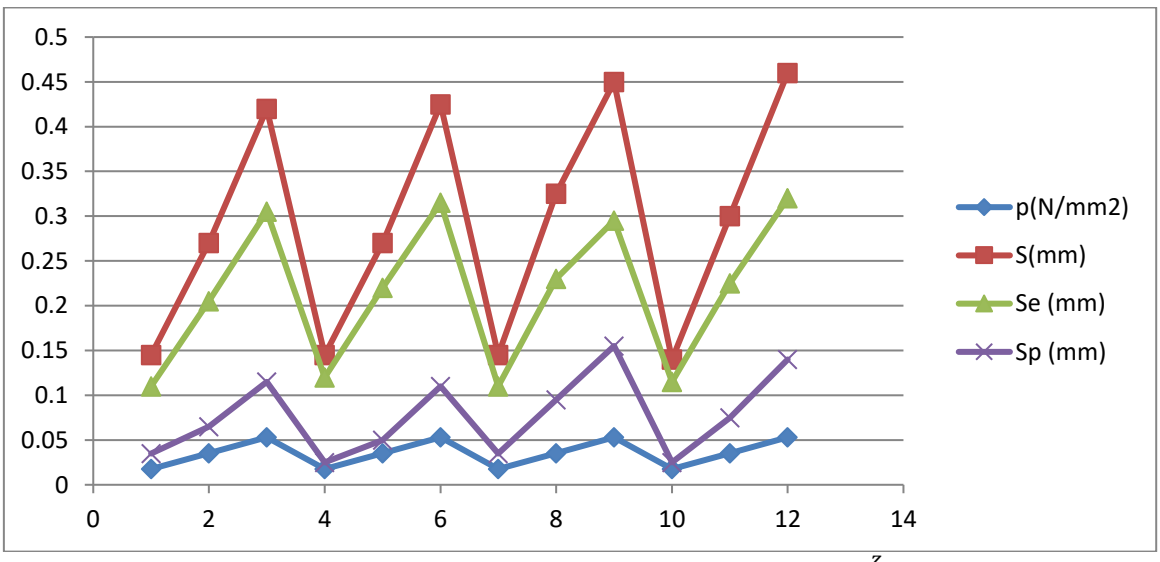

Figure 7. Periodic PLT on geocell reinforcement sand layer ($\frac{z}{d_{outer}} = 0.750$)

The figures above show the dynamic parameter values of the soilcomputed from experiential outputs of periodic plate-loading tests, which are performed on the geocell-reinforcement sand layer along different geocell-reinforcement conditions. All the results of predicting the bearing capacity of the sand layer in the presence of periodic loading are shown in Figures 5, 6 and 7. Monitoring the behavior of sandy soils under different types of loading can be enhanced by modern computerized cloud and internet of things system including modern microstrip antennas (sensors) and filters [25-32].

5. Conclusions

A series of cyclic loading tests have been carried out on four samples of sandy soils with different interior diameters. The samples have been loaded under the cyclic loading by frequencies which are different for the study effect of the reinforcing layers number and the frequency of cyclic loading on the behavior of soil samples. The attraction parameters of the soil-embedded reinforcement are adopted by such elements as the ability of the factors to resist tensile affairs, for example, tensile strength, the amount of the enchantment applied by tensile stress factors and the resistance of shear under the reinforcing and surrounding soil, for instance: A higher stress was computed by the soil interface that is reinforcement first reinforcement downward the soil. When the tensile force was found to be smaller concerning the factors, it broke off and became ineffective. If the tensile test is correct, but *isj* is the maximum in the expansion stress, then once the soil shows conditions higher due to the insufficient hardness of the method used for reinforcing the soil. Therefore, reinforced sand layers will have a capacity higher to support foundations exhibited to periodic and monotonous loading. For future work, more tests are required along various properties of the materials and the geometry shapes.
Moreover, the correct observation, such as the numerical technicality, was better for analyzing, including the parameters. The main conclusions are as follows: Including the geogrid can reduce the settlement and cumulative stress of samples under cyclic loading. The settlement and cumulative stress of samples increase with increasing frequency of loading. Samples tend to stabilize after about 1000 cycles of loading. The elastic parameters of the samples increase with cycles of loading. For samples with fewer reinforcing layers, the increment rate decreases faster than for those with more reinforcing layers. With the same number of reinforcing layers, the higher the load frequency, the lower the elastic modulus. With the same loading frequency, adding geogrid can exacerbate the rubber mold embedment effect of the samples. For the samples to have the same reinforcing layers while decreasing the frequency loading frequency, the significant increase in the effect of rubber mold embedding of sand samples As a recommendation for future research directions works, firstly; increasing numbers of layers to be more than even it will increase the coast of in term of materials and time but it will increase the reinforcement will give more accurate results and meet the main goal of this article. Secondly, using a mix of geogrid and cement increases the strength and stability of the soil.

Declaration of competing interest
The authors declare that they have no known financial or non-financial competing interests in any material discussed in this paper.

Funding information
No funding was received from any financial organization to conduct this research.

References

[1] S. K. Sasmal and R. N. Behera, "Transient settlement estimation of shallow foundation under eccentrically inclined static and cyclic load on granular soil using artificial intelligence techniques," *Geomechanics and Geoengineering*, pp. 1-17, 2022.

[2] Y. Peng, Z.-Y. Yin, C. Zhou, and X. Ding, "Micromechanical analysis of the capillary suction effect on bearing capacity of unsaturated fine granular foundation soil using coupled CFD-DEM method," *Computers and Geotechnics*, vol. 153, p. 105092, 2023.

[3] N. EsmaeilpourShirvani, A. TaghaviGhalesari, M. K. Tabari, and A. J. Choobbasti, "Improvement of the engineering behaviour of sand-clay mixtures using kenaf fibre reinforcement," *Transportation Geotechnics*, vol. 19, pp. 1-8, 2019.

[4] R. K. Mittal and G. Gill, "Sustainable application of waste tire chips and geogrid for improving load carrying capacity of granular soils," *Journal of Cleaner Production*, vol. 200, pp. 542-551, 2018.

[5] G. Cardile, M. Pisano, and N. Moraci, "The influence of a cyclic loading history on soil-geogrid interaction under pullout condition," *Geotextiles and Geomembranes*, vol. 47, no. 4, pp. 552-565, 2019.

[6] Q. Chen and M. Abu-Farsakh, "Ultimate bearing capacity analysis of strip footings on reinforced soil foundation," *Soils and Foundations*, vol. 55, no. 1, pp. 74-85, 2015.

[7] M. El Sawwaf and A. K. Nazir, "Behavior of repeatedly loaded rectangular footings resting on reinforced sand," *Alexandria Engineering Journal*, vol. 49, no. 4, pp. 349-356, 2010.

[8] A. M. Elleboudy, N. M. Saleh, and A. G. Salama, "Assessment of geogrids in gravel roads under cyclic loading," *Alexandria engineering journal*, vol. 56, no. 3, pp. 319-326, 2017.

[9] A. E. Elsaied, N. M. Saleh, and M. E. Elmashad, "Behavior of circular footing resting on laterally confined granular reinforced soil," *HBRC Journal*, vol. 11, no. 2, pp. 240-245, 2015.

[10] A. Hegde and T. Sitharam, "Experimental and numerical studies on footings supported on geocell reinforced sand and clay beds," *International Journal of Geotechnical Engineering*, vol. 7, no. 4, pp. 346-354, 2013.

[11] A. Hegde and T. Sitharam, "Behaviour of geocell reinforced soft clay bed subjected to incremental cyclic loading," *Geomechanics and Engineering*, vol. 10, no. 4, pp. 405-422, 2016.

[12] A. Hegde and T. Sitharam, "Experimental and numerical studies on protection of buried pipelines and underground utilities using geocells," *Geotextiles and Geomembranes*, vol. 43, no. 5, pp. 372-381, 2015.

[13] S. M. M. Najeeb, "Finding the discriminative frequencies of motor electroencephalography signal using genetic algorithm," *Telkomnika*, vol. 19, no. 1, pp. 285-292, 2021.

[14] O. Khalaj, N. J. Darabi, S. M. Tafreshi, and B. Mašek, "Protection of buried pipe under repeated loading by geocell reinforcement," in *IOP Conference Series: Earth and Environmental Science*, 2017, vol. 95, no. 2: IOP Publishing, p. 022030.

[15] G. M. Latha, S. K. Dash, and K. Rajagopal, "Numerical simulation of the behaviour of geocell reinforced sand in foundations," *International Journal of Geomechanics*, vol. 9, no. 4, pp. 143-152, 2009.

[16] R. M. Al_airaji, I. A. Aljazaery, and S. K. Al_dulaimi,"Generation of high dynamic range for enhancing the panorama environment," *Bulletin of Electrical Engineering and Informatics*, Article vol. 10, no. 1, pp. 138-147, 2021, doi: 10.11591/eei.v10i1.2362.

[17] K. Mamatha and S. Dinesh, "Performance evaluation of geocell-reinforced pavements," *International Journal of Geotechnical Engineering*, vol. 13, no. 3, pp. 277-286, 2019.

[18] S. K. Pokharel, J. Han, D. Leshchinsky, and R. L. Parsons, "Experimental evaluation of geocell-reinforced bases under repeated loading," *International Journal of Pavement Research and Technology*, vol. 11, no. 2, pp. 114-127, 2018.

[19] R. Sahu, R. Ayothiraman, and G. V. Ramana, "Dynamic response of model footing on reinforced sand," in *Geotechnical Earthquake Engineering and Soil Dynamics V: Slope Stability and Landslides, Laboratory Testing, and In Situ Testing*: American Society of Civil Engineers Reston, VA, 2018, pp. 199-207.

[20] S. Saride, V. K. Rayabharapu, and S. Vedpathak, "Evaluation of rutting behaviour of geocell reinforced sand subgrades under repeated loading," *Indian Geotechnical Journal*, vol. 45, pp. 378-388, 2015.

[21] L. Suku, S. S. Prabhu, P. Ramesh, and G. S. Babu, "Behavior of geocell-reinforced granular base under repeated loading," *Transportation Geotechnics*, vol. 9, pp. 17-30, 2016.

[22] S. M. Tafreshi and A. Dawson, "Behaviour of footings on reinforced sand subjected to repeated loading–Comparing use of 3D and planar geotextile," *Geotextiles and Geomembranes,* vol. 28, no. 5, pp. 434-447, 2010.

[23] H. Venkateswarlu, K. Ujjawal, and A. Hegde, "Laboratory and numerical investigation of machine foundations reinforced with geogrids and geocells," *Geotextiles and Geomembranes,* vol. 46, no. 6, pp. 882-896, 2018.

[24] J.-Q. Wang, L.-L. Zhang, J.-F. Xue, and Y. Tang, "Load-settlement response of shallow square footings on geogrid-reinforced sand under cyclic loading," *Geotextiles and Geomembranes,* vol. 46, no. 5, pp. 586-596, 2018.

[25]Y. S. Mezaal, H. T. Eyyuboglu, and J. K. Ali, "A novel design of two loosely coupled bandpass filters based on Hilbert-zz resonator with higher harmonic suppression," in *2013 Third International Conference on Advanced Computing and Communication Technologies (ACCT)*, 2013.

[26] S. A. Shandal, Y. S. Mezaal, M. F. Mosleh, and M. A. Kadim, "Miniaturized wideband microstrip antenna for recent wireless applications," *Adv. Electromagn.*, vol. 7, no. 5, pp. 7–13, 2018.

[27] Y. S. Mezaal and H. T. Eyyuboglu, "A new narrow band dual-mode microstrip slotted patch bandpass filter design based on fractal geometry," in *7th International Conference on Computing and Convergence Technology (ICCIT, ICEI and ICACT)*, 2012, pp. 1180–1184.

[28] Y. S. Mezaal, H. H. Saleh, and H. Al-saedi, "New compact microstrip filters based on quasi fractal resonator," *Adv. Electromagn.*, vol. 7, no. 4, pp. 93–102, 2018.

[29] F. Abayaje, S. A. Hashem, H. S. Obaid, Y. S. Mezaal, and S. K. Khaleel, "A miniaturization of the UWB monopole antenna for wireless baseband transmission," *Periodicals of Engineering and Natural Sciences,* vol. 8, no. 1, pp. 256–262, 2020.

[30] Y. S. Mezaal and J. K. Ali, "Investigation of dual-mode microstrip bandpass filter based on SIR technique," *PLoS One*, vol. 11, no. 10, p. e0164916, 2016.

[31]T. Abd, et al., "Iraqi e-government and cloud computing development based on unified citizen identification," *Periodicals of Engineering and Natural Sciences*, vol. 7, no. 4, pp. 1776 - 1793, 2019.

[32] A. A H. Mohamad, Y. S. Mezaal, and S. F. Abdulkareem, "Computerized power transformer monitoring based on internet of things," *Int. J. Eng. Technol.*, vol. 7, no. 4, p. 2773, 2018.